

Hyperfine structure in the metastable D states of atomic barium

Stephen G. Schmelling

Department of Physics and Astronomy, State University of New York at Buffalo, Buffalo, New York 14214

(Received 29 October 1973)

The atomic-beam magnetic-resonance method has been used to measure the magnetic dipole and electric quadrupole hyperfine-structure interaction constants A and B for the 3D_3 , 3D_2 , and 1D_2 states of the $\dots(6s)(5d)$ configuration for ${}^{135}\text{Ba}$ and ${}^{137}\text{Ba}$. The experimental results for ${}^{135}\text{Ba}$ are $A({}^1D_2) = -73.429(4)$ MHz, $B({}^1D_2) = +38.710(15)$ MHz, $A({}^3D_2) = +370.6(7)$ MHz, $B({}^3D_2) = +18.3(22)$ MHz, $A({}^3D_3) = +408.1(14)$ MHz, $B({}^3D_3) = +20(8)$ MHz; and for ${}^{137}\text{Ba}$, $A({}^1D_2) = -82.180(3)$ MHz, $B({}^1D_2) = +59.564(14)$ MHz, $A({}^3D_2) = +413.9(9)$ MHz, $B({}^3D_2) = +26.8(30)$ MHz, $A({}^3D_3) = +455.4(16)$ MHz, $B({}^3D_3) = +36(9)$ MHz. A comparison is made between the value of the electric quadrupole moment of the ${}^{137}\text{Ba}$ nucleus obtained from these results, which depend on the interaction of the $5d$ electron, and the value obtained from earlier results, which depend on the interaction of the $6p$ electron. There is a substantial difference in the values of $Q({}^{137}\text{Ba})$ obtained from these two sets of measurements if one does not take the quadrupole shielding into account. Taking the quadrupole shielding into account markedly reduces this difference.

I. INTRODUCTION

During the past ten or so years, the detailed properties of the lower-lying electronic states of atomic barium have been extensively studied. Radiative lifetimes,¹⁻⁴ electronic g factors,^{2,5,6} and the hyperfine structure^{1,6-8} (hfs) of some of the states of the $(6s)(6p)$ configuration have been studied by various optical techniques. A number of other investigations have also been made of the hfs in sp configurations in several species, but little detailed work has been done on the hfs of the terms of an sd configuration. In a situation unique to barium, all the terms arising from the lowest sd configuration are metastable and are amenable to study by atomic-beam magnetic-resonance (ABMR) techniques⁹ as well as optical techniques.¹⁰ This paper is a report of an ABMR study of the hfs of the 1D_2 , 3D_3 , and 3D_2 terms of the $(6s)(5d)$ configuration of ${}^{137}\text{Ba}$ and ${}^{135}\text{Ba}$.

In addition to providing general information on the nature of the hfs interaction in a configuration of the sort $(ns)(n'd)$, these measurements can provide information on the relative size of the quadrupole shielding factors for the $5d$ and $6p$ electrons. As is shown below, if one neglects the quadrupole shielding factors, the value of the nuclear quadrupole moments of ${}^{137}\text{Ba}$ and ${}^{135}\text{Ba}$ obtained from these measurements on the interaction of the $5d$ electron with the barium nucleus are in substantial disagreement with the values of the quadrupole moments obtained from measurements on the interaction of the $6p$ electron.^{1,6-8,11} Taking account of these correction factors markedly reduces the disagreement.

II. THE EXPERIMENT

A. General procedures

The lowest-lying electronic levels of Ba I are shown in Fig. 1. The ground-state configuration is $\dots(6s)^2$ and has no hfs interaction. The first excited configuration $\dots(6s)(5d)$ gives rise to the states 1D_2 , 3D_3 , 3D_2 , and 3D_1 . Since all these states lie below the states of the configuration $\dots(6s)(6p)$, they cannot readily decay by radiative transitions. The fact that they can be detected in an ABMR experiment means that their radiative lifetime must be greater than 1 msec.

If one ignores interactions which are off-diagonal in J , the electronic angular momentum, the interaction Hamiltonian for a free atom in a uniform magnetic field is

$$H = hA\vec{I} \cdot \vec{J} + hB \left(\frac{3(\vec{I} \cdot \vec{J})^2 + \frac{3}{2}(\vec{I} \cdot \vec{J}) - I(I+1)J(J+1)}{2I(2I-1)J(2J-1)} \right) - g_J \mu_B \vec{J} \cdot \vec{H} - g_I \mu_B \vec{I} \cdot \vec{H}. \quad (1)$$

In Eq. (1), I and J are respectively the nuclear and electronic angular-momentum operators, A and B are the magnetic-dipole and electric-quadrupole hyperfine interaction constants, μ_B is the Bohr magneton, h is Planck's constant, and g_I and g_J are respectively the nuclear and electronic g factors in terms of the Bohr magneton. Equation (1) also neglects the octupole interaction.

The basic experimental technique used here is the standard ABMR technique in which atoms effuse from an oven, pass successively through three magnets labeled A , C , and B , and impinge

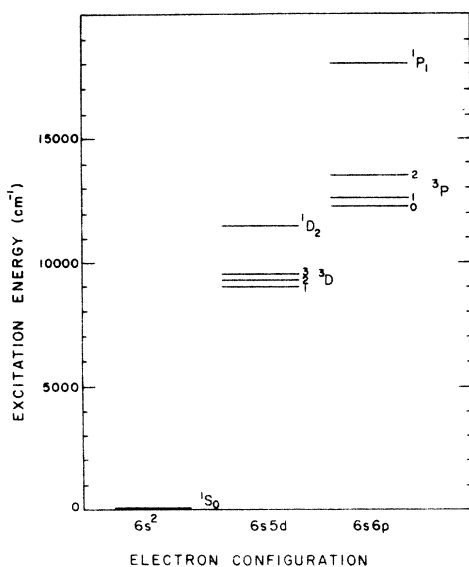


FIG. 1. Low-lying electronic states of Ba I.

on a detector. The *A* and *B* magnets are inhomogeneous deflecting magnets. If the sign of the effective magnetic moment is reversed in the homogeneous *C* magnet, the atoms in the beam are deflected towards the detector; if not, they are deflected away from it. In the *C* magnet the beam atoms interact with a weak rf magnetic field. If the frequency of the rf field corresponds to the difference in energy between two appropriate Zeeman levels of the atom, the necessary reversal of the sign of the effective magnetic moment takes place, which results in an increase in the number of atoms reaching the detector. One can then fit the measured resonant frequencies to Eq. (1) to determine the hfs parameters *A* and *B*.

B. Apparatus

The atomic-beam apparatus used in this experiment is similar to one previously described in the literature¹² and will not be discussed in detail here. It uses a six-pole *A* magnet and a two-pole *B* magnet, both of which are permanent magnets. The *C* magnet is a Hall-probe-regulated variable electromagnet. All the magnets are located inside the vacuum envelope of the apparatus.

The beam of metastable barium atoms was produced by a dual electron bombardment technique which was a modification of the technique used by Brink and Hull.⁹ A sample of metallic barium was placed in a steel oven with a circular orifice in one side of it. Electrons emitted by one filament, stretched across the top of the oven, were primarily used to heat the oven. Electrons emitted by a second filament, hung in a loop below the

oven orifice, were used both to heat the oven and to excite the barium atoms as they emerged from the oven. The two filaments could be independently biased with respect to the oven and each other. When the exciting filament was being used one could see an intense light at the oven orifice. This fact, coupled with the intensity of the metastable beam, seemed to imply that the excitation took place in a discharge in the short exit channel of the oven! We estimate that (10–20)% of the barium beam was excited into metastable states.

The *A* magnet deflects atoms with negative effective magnetic moments toward the axis of the beam machine and atoms with positive effective magnetic moments out toward the pole pieces of the magnet. The *B* magnet deflects atoms with positive magnetic moments towards the detector and those with negative magnetic moments away from it. Metastable barium has integral electronic angular momentum, and there are states for which the effective magnetic moment is zero. Under certain conditions, atoms whose effective magnetic moment is zero in either the *A* or *B* magnet can also reach the detector. However, for the particular set of experimental conditions under which this experiment was carried out, atoms whose effective magnetic moment was zero in either the *A* or *B* magnet did not give rise to signals which were large enough to be useful.

The barium beam was detected by surface ionization on a set of tungsten filaments followed by mass analysis by a Paul mass filter and an electron multiplier. The ionization potential of metastable barium is less than the work function of tungsten, so that the surface ionization is very efficient. In point of fact, it is also possible to detect ground-state barium atoms with reasonable efficiency by surface ionization, even though the ionization potential (5.2 eV) is somewhat higher than the work function of tungsten. We ran the filaments at about 1800 °C to minimize the sticking time of the barium on the filaments.

Data were recorded by a digital signal averaging system built around a Data General Supernova computer. Pulses from the electron multiplier are stored in the memory of the computer which repeatedly scans through the resonance. In this experiment, the procedure was to set the *C*-magnet field at a particular value and scan the frequency. The computer was programmed to allow one to vary the rate of scanning, the size of the frequency increments, the total number of scans, and so on, in order to optimize the signal-to-noise ratio.

Radio frequencies below 70 MHz were produced directly by amplifying the output of a General Radio 1164-A frequency synthesizer. Frequencies between 70 and 500 MHz were obtained by multiply-

ing the output of the frequency synthesizer, and then amplifying the output of the multiplier with a tuned amplifier. The rf hairpin was either a shorted coaxial line or a U-shaped copper strap.

C. Experimental procedure

The general procedure for measuring a hfs interaction by ABMR is to follow one or more of the $\Delta F=0$ ($\vec{F}=\vec{I}+\vec{J}$) transitions as a function of magnetic field, using the deviation from the linear Zeeman effect to determine the hfs intervals. One can then use the values of the hfs intervals determined in this way as the starting point for a direct measurement of the hfs interval by observation of a $\Delta F=\pm 1$ transition.

Figure 2 shows the energy levels of the 1D_2 state of ^{137}Ba as a function of magnetic field. The $\Delta F=0$ transitions that were observed are labeled α and β . Because barium has integral J , the only $\Delta F=0$ transitions which can readily be observed in our beam machine are two quantum transitions with $\Delta M_F = -2$. As one goes to higher and higher magnetic fields, such transitions require increasingly higher rf power levels and eventually become unobservable. With our apparatus we could observe such two quantum transitions until the difference in frequency between the two single-quantum transitions was a few MHz.

The beam of metastable barium atoms was pro-

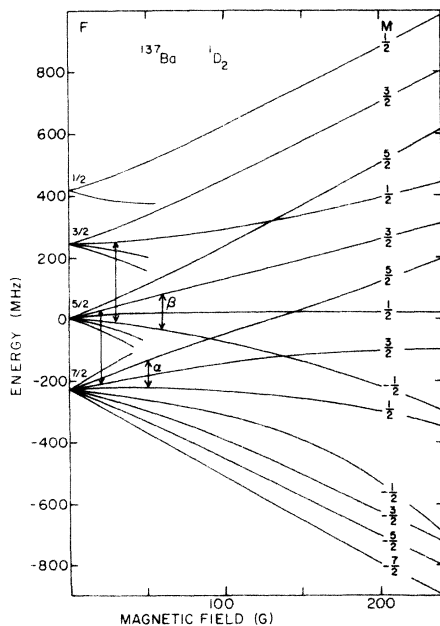


FIG. 2. Energy vs magnetic field for the Zeeman hyperfine levels of the 1D_2 state of ^{137}Ba . The observed transitions are indicated by the arrows.

duced by heating and exciting a sample of barium metal with the natural isotopic composition in the manner described above. The natural isotopic abundances of ^{135}Ba and ^{137}Ba are 6.6% and 11.3%, respectively. This fact, plus the requirement that the beam had to be excited by electron bombardment to produce the metastable states, meant that only a small fraction of the total atomic beam was in the states of interest, and necessitated the use of the signal averaging techniques.

The usual procedure was to scan through a resonance at a rate of 0.01 sec per channel, incrementing the frequency in steps of 4 to 8 kHz per channel. Good signals could typically be seen after 500 to 1000 scans over a resonance. An example of a $\Delta F=+1$ resonance in the 1D_2 state of ^{137}Ba is shown in Fig. 3.

The C field was calibrated by observing $\Delta J=0$ transitions between the Zeeman levels of the 3D_2 or 1D_2 states of the even mass barium isotopes, principally ^{138}Ba . These isotopes have no hfs and have an isotopic abundance of 82%. Signals from the even mass isotopes could typically be seen with a signal-to-noise ratio of 3:1 after one scan through the resonance. The electronic g factors used to calculate the field are those of von Oppen.¹⁰

For the 1D_2 state we observed $\Delta F=0$ resonances at several values of magnetic field, and then using the results of these observations we searched for and observed $\Delta F=+1$ transitions at low values of magnetic field to obtain precise values of A and B . For the 3D_3 and 3D_2 states we observed $\Delta F=0$

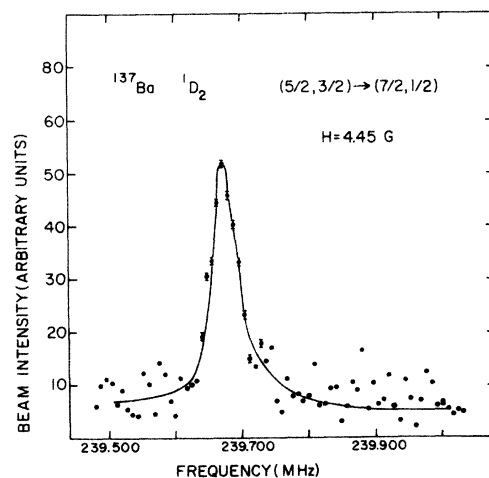


FIG. 3. $\Delta F=-1$ resonance in the 1D_2 state of ^{137}Ba . For the points without error bars, the size of the statistical uncertainty is of the order of the size of the dot. The jitter in the baseline is probably due to fluctuations in the source discharge.

transitions out to a field of about 150 G. We did not search for the $\Delta F = -1$ transitions in these states because the necessary rf equipment was not available to us. In all cases data were taken for both ^{137}Ba and ^{135}Ba . Signals from the 3D_1 state were too small to permit a measurement of the hfs of this state.

The Berkeley computer program HYPERFINE-68 was then used to determine A and B by making a least-squares fit of the data to Eq. (1), treating A and B as variable parameters. In making the least-squares fit, the values of the nuclear g factor used were taken from Fuller and Cohen.¹³

III. DATA ANALYSIS

A. Results

The results of the least-squares fit are shown in Table I. The values labeled "uncorrected" are obtained directly from the output of the least-squares fit. The "corrected" values are explained below. Within the experimental uncertainties the values for the ratios of the A 's and B 's for ^{137}Ba to those for ^{135}Ba are the same for all three states.

The theory of the hfs of an sl configuration was first worked out years ago by Breit and Wills.¹⁴ Later, Lurio, Mandel, and Novick¹⁵ (referred to as LMN) showed how one can extend the theory to take into account the second-order corrections to the hfs due to interactions between the different J states of an L - S multiplet.

For the 3D_3 , 3D_2 , and 1D_2 states of an sd configuration, one can write the parameters A and B of Eq. (1) in terms of one-electron hfs parameters as follows¹⁵:

$$A(^3D_3) = \frac{1}{6}a_s + \frac{5}{8}a_{5/2}, \quad (2a)$$

$$A(^3D_2) = \left(\frac{1}{4}c_2^2 - \frac{1}{8}c_1^2\right)a_s + \frac{7}{8}c_1^2a_{5/2} + \frac{3}{4}c_2^2a_{3/2} - (7/24\sqrt{6})\xi c_1c_2a_{5/2}, \quad (2b)$$

$$A(^1D_2) = \left(\frac{1}{4}c_1^2 - \frac{1}{8}c_2^2\right)a_s + \frac{7}{8}c_2^2a_{5/2} + \frac{3}{4}c_1^2a_{3/2} + (7/24\sqrt{6})\xi c_1c_2a_{5/2}, \quad (2c)$$

and

$$B(^3D_3) = b_{5/2}, \quad (2d)$$

$$B(^3D_2) = \frac{4}{5}c_1^2b_{5/2} + c_2^2b_{3/2} - \sqrt{\frac{6}{5}}\eta c_1c_2b_{5/2}, \quad (2e)$$

$$B(^1D_2) = \frac{4}{5}c_2^2b_{5/2} + c_1^2b_{3/2} + \sqrt{\frac{6}{5}}\eta c_1c_2b_{5/2}. \quad (2f)$$

Here, a_s is the dipole coupling constant for the s electron, and $a_{5/2}$ and $b_{5/2}$, and $a_{3/2}$ and $b_{3/2}$, are the dipole and quadrupole coupling constants for the d electron in the $j = \frac{5}{2}$ and $j = \frac{3}{2}$ states, respectively. They are defined, for example, in LMN. In the limit of no configuration interaction, the a_j 's and b_j 's would be the same for the triplet and singlet states. The validity of this assumption is discussed below. The parameters ξ and η are relativistic correction factors whose values are close to 1. They are defined by Schwartz.¹⁶ The parameters c_1 and c_2 are the intermediate coupling coefficients for the 3D_2 and 1D_2 states. For metastable barium, values of c_1 and c_2 needed to calculate electronic g factors in agreement with experiment are given by Brink and Hull.⁹ We use these values in our subsequent data analysis. In addition to the above relationships, the definitions of the a_j 's and b_j 's imply that

$$a_{3/2} = \frac{7}{3}(F_{3/2}/F_{5/2})a_{5/2} \quad (3a)$$

and

$$b_{3/2} = \frac{7}{10}(R_{3/2}/R_{5/2})b_{5/2}, \quad (3b)$$

where the F_j 's and the R_j 's are the relativistic correction factors of Casimir.¹⁷

The experimental data were analyzed in the following way for ^{137}Ba . First, it was assumed that $a_{5/2}$ and a_s were the same for the 3D_3 and 3D_2 states. Then, using Eqs. (2a), (2b), and (3a)

TABLE I. Values of the hyperfine-structure interaction constants. The "uncorrected" values are taken directly from the output of the least-squares fit. The "corrected" values have been corrected for the second-order hfs interactions between states of the $6s5d$ configuration.

Isotope and State	A (uncorrected) (MHz)	A (corrected) (MHz)	B (uncorrected) (MHz)	B (corrected) (MHz)
$^{137}\text{Ba } ^1D_2$	-82.180(3)	-82.229	+59.564(14)	+59.759
$^{137}\text{Ba } ^3D_2$	+413.9(9)	+414.0	+26.8(30)	+27.0
$^{137}\text{Ba } ^3D_3$	+455.4(16)	+455.4	+36(9)	+36
$^{135}\text{Ba } ^1D_2$	-73.429(4)	-73.471	+38.710(15)	+38.830
$^{135}\text{Ba } ^3D_2$	+370.6(7)	+370.3	+18.3(22)	+18.5
$^{135}\text{Ba } ^3D_3$	+408.1(14)	+408.1	+20(8)	+20

and the experimental values of $A(^3D_3)$ and $A(^3D_2)$, we determined a value for $a_{5/2}$ and a_s . This value of a_s was assumed to be the same for the triplet and singlet states, and was used to extract a second value of $a_{5/2}$ using Eq. (2c) and (3a) and the experimental value of $A(^1D_2)$. For each value of $a_{5/2}$, one for the triplet states and one for the singlet state, one can obtain a value of $\langle r^{-3} \rangle_{5d}$. These results are shown in Table II. The agreement between the triplet and singlet values of $a_{5/2}$ and $\langle r^{-3} \rangle_{5d}$ is quite good, and possibly fortuitous, considering the neglect of any explicit attempt to account for such effects as configuration interaction.

The values of $\langle r^{-3} \rangle_{5d}$ thus obtained were also used with Eqs. (2d), (2e) and (2f), and Eq. (3b), and the experimental values of the quadrupole hfs constants B to obtain a value for the quadrupole moment of ^{137}Ba . The quadrupole moment of ^{135}Ba could be obtained from the ratio of the quadrupole coupling constants.

Finally, the values of the a_j 's and the b_j 's were used to calculate the second-order corrections to the measured values of A and B , using the formulas of LMN. For the 1D_2 state these corrections are substantially larger than the experimental errors. For the 3D_3 and 3D_2 states, the corrections are smaller than the experimental errors. In either case, these second-order corrections caused no significant change in the one-electron parameters a_j and b_j , so that it was not necessary to redo the whole calculation in an iterative manner.

B. Quadrupole moment of ^{137}Ba

The values of the nuclear electric quadrupole moment of ^{137}Ba obtained from the quadrupole coupling constants B by the method described above are

$$^1D_2: Q = +0.42(1) \times 10^{-24} \text{ cm}^2,$$

$$^3D_2: Q = +0.37(4) \times 10^{-24} \text{ cm}^2,$$

$$^3D_3: Q = +0.28(7) \times 10^{-24} \text{ cm}^2.$$

The errors quoted for the 3D_2 and 3D_3 states

TABLE II. Values of the one-electron magnetic hfs parameters. The parameter a_s is assumed to be the same for both the triplet and singlet states.

State	a_s (MHz)	$a_{5/2}$ (MHz)	$\langle r^{-3} \rangle_{5d}$ (a_0^{-3})
$^3D_3, ^3D_2$	2530	39.5	0.910
1D_2	2530	42.0	0.970

represent experimental errors in the measured values of the hfs constants, while the quoted error for the 1D_2 state derives from the uncertainties in the procedure for obtaining A from B . The agreement between these values of Q is marginal but probably not completely unreasonable when one considers the assumptions that have gone into extracting these numbers from the interaction constants. For example, the assumption that a_s is the same in the singlet and triplet states is certainly open to question. Moreover, similar discrepancies have been found for the value of $A(^{137}\text{Ba})$ obtained from measurements on the 3P_1 state⁷ and the 1P_1 state.^{1,8} All of these values of $Q(^{137}\text{Ba})$ are uncorrected for quadrupole shielding effects. If one uses a value of $\langle r^{-3} \rangle_{5d}$ based on the fine structure of the D states, the above values for $Q(^{137}\text{Ba})$ are increased by about 15%.

As mentioned above, there have been several previous measurements^{1,7,8,11} of $Q(^{137}\text{Ba})$ based on the hfs interaction of the $6p$ electron. One can compare values of $Q(^{137}\text{Ba})$ with these values. zu Putlitz⁷ finds $Q(^{137}\text{Ba}) = +0.28(3) \times 10^{-24} \text{ cm}^2$ from measurements on the hfs of the 3P_1 state, Becker *et al.*¹¹ find $Q(^{137}\text{Ba}) = +0.26(3) \times 10^{-24} \text{ cm}^2$ from measurements on the Ba II spectrum, Jackson and Tuan⁸ find $Q(^{137}\text{Ba}) = +0.21(5) \times 10^{-24} \text{ cm}^2$ from measurements on the hfs of the Ba I resonance line, and Lurio¹ finds $Q(^{137}\text{Ba}) = \pm 0.20 \times 10^{-24} \text{ cm}^2$ from measurements on the hfs of the 1P_1 state. Our most reliable value is $Q(^{137}\text{Ba}) = +0.42(1) \times 10^{-24} \text{ cm}^2$ based on the 1D_2 hfs. Neglecting the quadrupole shielding leaves the values of $Q(^{137}\text{Ba})$ obtained from the measurements on the D states and the P states in substantial disagreement.

The quadrupole shielding factor R is defined by $Q = Q'/(1 - R)$, where Q is the value one would measure in the absence of shielding and Q' is the actual measured value. For the $5d$ electron, Sternheimer¹⁸ gives $R = -0.4 \pm 0.1$, giving $1/(1 - R) = 0.71$ and

$$Q(^{137}\text{Ba}, 5d) = +0.30 \times 10^{-24} \text{ cm}^2,$$

using the value of $Q(^{137}\text{Ba})$ derived from the 1D_2 hfs. For the $6p$ electron, Murakawa¹⁹ gives $R = -0.1$, giving $1/(1 - R) = 0.90$, and

$$Q(^{137}\text{Ba}, 6p) = +0.25 \times 10^{-24} \text{ cm}^2,$$

using the results of zu Putlitz.⁷

The corrected values are thus in much better agreement than the uncorrected values, although there are still differences between the values of the quadrupole moments derived from different measurements that are much larger than the experimental errors associated with the measured values of the quadrupole interaction constants.

ACKNOWLEDGMENTS

I would like to thank Stephan Heider for his efforts in designing and building the data acquisition system, Gilbert Brink for help in several phases

of the experiment, and Manuel Perez for his assistance in some of the early phases of this work. I would also like to thank Dr. R. M. Sternheimer for a helpful communication on the quadrupole shielding factors.

-
- ¹A. Lurio, *Phys. Rev.* 136, A376 (1964).
²M. W. Swagel and A. Lurio, *Phys. Rev.* 169, 114 (1968).
³L. O. Dickie and F. M. Kelly, *Can. J. Phys.* 49, 2630 (1971); 49, 1098 (1971); 48, 879 (1970).
⁴P. Schenck, R. C. Hilborn, and H. Metcalf, *Phys. Rev. Lett.* 31, 189 (1973).
⁵I. J. Ma, J. Mertens, G. zu Putlitz, and G. Schütte, *Z. Phys.* 208, 266 (1968).
⁶G. von Oppen, *Z. Phys.* 213, 254 (1968).
⁷G. zu Putlitz, *Ann. Phys.* 11, 248 (1963).
⁸D. A. Jackson and D. A. Tuan, *Proc. Phys. Soc. Lond. A* 280, 323 (1964).
⁹G. O. Brink and R. J. Hull, *Phys. Rev.* 179, 43 (1969).
¹⁰G. von Oppen, *Z. Phys.* 213, 261 (1968); G. von Oppen and B. Piosczyk, *Z. Phys.* 229, 163 (1969).
¹¹W. Becker, W. Fischer, and H. Hühnermann, *Z. Phys.* 216, 142 (1968).
¹²R. J. Hull and G. O. Brink, *Phys. Rev. A* 1, 685 (1970).
¹³G. H. Fuller and V. W. Cohen, *Nuclear Data* 5, 433 (1969).
¹⁴G. Breit and L. A. Wills, *Phys. Rev.* 44, 470 (1933).
¹⁵A. Lurio, S. Mandel, and R. Novick, *Phys. Rev.* 126, 1758 (1972).
¹⁶C. Schwartz, *Phys. Rev.* 97, 380 (1955).
¹⁷H. Kopferman, *Nuclear Moments* (Academic, New York, 1958).
¹⁸R. M. Sternheimer, *Phys. Rev. A* 6, 1702 (1972); *Phys. Rev.* 164, 10 (1967); and private communication.
¹⁹K. Murakawa, *Phys. Rev. A* 7, 416 (1973).